Chemical Sinks of Organic Aerosol: Kinetics and Products of the Heterogeneous Oxidation of Erythritol and Levoglucosan

Citation: Kessler, Sean H. et al. "Chemical Sinks of Organic Aerosol: Kinetics and Products of the Heterogeneous Oxidation of Erythritol and Levoglucosan." Environmental Science & Technology 44.18 (2010): 7005–7010. Web.

As Published: http://dx.doi.org/10.1021/es101465m

Publisher: American Chemical Society

Persistent URL: http://hdl.handle.net/1721.1/71705

Version: Author's final manuscript: final author's manuscript post peer review, without publisher's formatting or copy editing

Chemical sinks of organic aerosol: kinetics and products of the heterogeneous oxidation of erythritol and levoglucosan

Sean H. Kessler,[1] Jared D. Smith,[2] Dung L. Che,[2,3] Douglas R. Worsnop,[4] Kevin R. Wilson,[2] Jesse H. Kroll*[1,5]

[1] *Department of Chemical Engineering, Massachusetts Institute of Technology, Cambridge MA 02139;* [2]*Chemical Sciences Division, Lawrence Berkeley National Laboratory, Berkeley CA 94720;* [3]*Department of Chemistry, University of California, Berkeley, CA 94720;* [4]*Center for Aerosol and Cloud Chemistry, Aerodyne Research Inc., Billerica MA 01821;* [5] *Department of Civil and Environmental Engineering, Massachusetts Institute of Technology, Cambridge MA 02139*

I. Abstract

The heterogeneous oxidation of pure erythritol ($C_4H_{10}O_4$) and levoglucosan ($C_6H_{10}O_5$) particles was studied in order to evaluate the effects of atmospheric aging on the mass and chemical composition of atmospheric organic aerosol. In contrast to what is generally observed for the heterogeneous oxidation of reduced organics, substantial volatilization is observed in both systems. However, the ratio of the decrease in particle mass to the decrease in the concentration of the parent species is about three times higher for erythritol than for levoglucosan, indicating that details of chemical structure (such as carbon number, cyclic moieties, and oxygen-containing functional groups) play a governing role in the importance of volatilization reactions. The kinetics of the reaction indicate that while both compounds react at approximately the same rate, reactions of their oxidation products appear to be slowed substantially. Estimates of volatilities of organic species based on elemental composition measurements suggest that the

heterogeneous oxidation of oxygenated organics may be an important loss mechanism of organic aerosol.

II. Introduction

Atmospheric organic aerosol (OA) is of special concern in considering the effects of particulate matter on human health and global radiative forcing. Quantitative predictions of OA loadings and properties often fail to match ambient measurements, in large part because of the highly complex nature of organic mixtures and because the continuing oxidative aging of organics during their atmospheric lifetimes (*1*). These oxidation reactions may occur either in the vapor phase, as with volatile or semivolatile organics, or by heterogeneous reactions at the gas-particle interface (*2*,*3*,*4*,*5*,*6*).

Recent laboratory work has focused on the heterogeneous oxidation of model condensed-phase organic species, in order to understand the role of such reactions in aging mechanisms of primary organic aerosol. Several studies (*2*,*3*,*5*) have found that substantial oxidation of reduced organics, as well as loss of OA mass, occurs only at very high oxidant exposures, beyond what most particles will experience in their atmospheric lifetimes. Nonetheless, this work suggests that oxidized organics may be susceptible to volatilization reactions; these may be atmospherically important given the abundance of oxidized compounds in OA (*1*).

In this study we investigate the kinetics and products of the heterogeneous oxidation of oxygenated (polyhydroxylated) species by exposure to hydroxyl (OH) radicals. We focus on two model organics, chosen both for their high degree of oxidation and for their importance as surrogate or tracer species in OA. Erythritol, $C_4H_{10}O_4$, is an analog of 2-methyl erythritol, a tracer species for isoprene secondary OA (SOA) (*7*,*8*). Levoglucosan, $C_6H_{10}O_5$, is a known product of cellulose pyrolysis and is frequently used as a tracer for biomass burning OA (BBOA)

(*9*). Although the role of these compounds in atmospheric chemistry differs greatly, they are functionally similar, with low carbon numbers, several hydroxyl groups, and a relatively high degree of oxygenation (oxygen-to-carbon ratios of 0.8 to 1.0). The rates of oxidation of both species may strongly affect their efficacy as tracers in determining relative amounts of SOA and BBOA (*10,11,12,13*). More generally, the goal of this work is to investigate the possibility that oxidative aging of organic aerosol may serve as a chemical sink of atmospheric particulate matter (PM) via formation of volatile products (*14*).

III. Experimental Methods

The flow reactor used to study the heterogeneous oxidation of particles has been described in detail previously (*4,5*) and will be discussed only briefly here. The reactor is made up of type-219 quartz, with a length of 130 cm, inner diameter of 2.5 cm, and residence time of ~37 s. Carrier flow consists of an O_2/N_2 mixture (in a 5/95 volume ratio), humidified to 30% RH. Organic aerosol is generated by sending an aqueous solution of each organic through either a constant-output atomizer (erythritol, >99% purity, Aldrich) (*15*) or a commercial nebulizer (levoglucosan, 99% purity, Aldrich) (*16*), and the resulting particles (surface-weighted mean diameter of ~270-305 nm) are drawn through a diffusion drier and into the flow reactor at loadings of ~500-750 $\mu g\ m^{-3}$. Such loadings are sufficiently high to ensure that >95% of the erythritol and >99% of the levoglucosan is present in the condensed phase at equilibrium.

Ozone is produced by either a mercury pen-ray lamp (1-10 ppm) or a commercial corona discharge ozone generator (10-200 ppm, OzoneLab Instruments). O_3 concentrations, which determine the level of OH exposure within are determined using an ozone monitor (2B Technologies Inc.). Within the flow reactor (temperature: 35 ºC), ozone is photolyzed by UV light at 254 nm from two mercury lamps positioned immediately outside the quartz tube. $O(^1D)$

generated by ozone photolysis subsequently reacts with water vapor to form a pair of hydroxyl radicals (OH), which initiate oxidation of the particles. The water vapor concentration is maintained at a sufficiently high level to ensure that direct oxidation of organics by $O(^1D)$ is negligible, as determined previously (*5*). Hexane (~100 ppb) added to the tube is monitored by GC-FID to quantify OH concentration. This technique has been used to correctly predict rate constants in the reaction of OH with other selected gas-phase organics (*4*,*5*); OH concentrations, which are changed by varying O_3, range from 10^9 to 2×10^{11} molecule cm^{-3}. Such concentrations correspond to approximate atmospheric exposures of 1 day to four weeks, assuming an average ambient OH concentration of 3×10^6 molecule cm^{-3}. It should be cautioned that these high OH concentrations may lead to significant secondary chemical effects, which would make linear extrapolation to ambient levels highly uncertain. Examination of these secondary effects by comparison of low- and high-concentration experiments at varying residence times is therefore an important topic for future research.

Particles exiting the flow reactor are sampled into a scanning mobility particle sizer (SMPS, TSI, Inc.), for the measurement of particle mobility diameters, and a high-resolution time-of-flight aerosol mass spectrometer (HR-ToF-AMS, Aerodyne Research, Inc.), for the measurement of particle composition (operating in "W-mode") and vacuum aerodynamic diameter ("V-mode"). Particle mass is obtained from combined SMPS measurements and AMS particle-time-of-flight (PToF) data, by multiplying average particle volume (from the SMPS) by the effective particle density (Figure S-2). Although this is strictly valid only for spherical particles, minor variations in particle shape will result in only small errors in measured mass, less than 10% (*17*).

Pure particles of levoglucosan and erythtritol did not change in composition or mass when the UV lights were turned on but no ozone was added, verifying both that the parent organic compounds studied are not directly photolyzed, and that UV-generation of condensed-phase oxidants is negligible. Significant gas-phase oxidation of the semivolatile compounds studied here is also highly unlikely, due to their strong partitioning into the particle phase and the short residence time in the flow reactor. Thus any changes to the mass or composition of the particles result from heterogeneous oxidation of particulate species by gas-phase OH radicals.

The amount of starting compound (levoglucosan or erythritol) lost by reaction is quantified by selecting a marker peak from the high-resolution mass spectrum and computing its fractional contribution to total AMS mass:

$$m_j = \frac{i_j}{i_{total}} m_{OA} \quad (1)$$

where i_j is the peak signal of the fragment ion selected to represent compound j, i_{total} is the sum of all organic peak signals from the AMS, and m_{OA} is the OA mass, normalized by particle number in order to account for wall losses, small atomizer fluctuations, and changes in collection efficiency of the AMS. This method assumes that the chosen marker peak does not constitute a significant portion of the individual mass spectra of the oxidation products, so that the peak represents only the compound of interest. This approach has recently been shown to compare very well with offline techniques for quantifying levoglucosan (*10*).

The peak used to track the mass loss of erythritol is chosen to be $C_4H_8O_3^+$ (*m/z* = 104), which is formed by the neutral loss of H_2O from the molecular ion (M-18). Likewise, the selected marker peak for levoglucosan is $C_6H_8O_4^+$ (*m/z*=144), also obtained by the loss of H_2O. Both peaks were observed to be the fragments of highest mass in the pure compound spectra for

which the AMS signal-to-noise ratio was suitably large. It is unlikely that any oxidation products would contribute significantly to the selected peaks, since they are expected to be of lower mass (aside from oligomerization products, which are not strongly represented in these AMS spectra) and have fewer hydrogen atoms than the parent compound.

The effects of oxidation by OH exposure may vary widely, depending on the nature of the organic compound being oxidized. It is therefore useful to introduce the mass loss ratio (MLR), defined as the ratio of the change in particle mass to the change in mass of the reacting species. For a given particle mass m_{OA}, reactive species mass m_R, and particles initially composed of the pure reactive species, such that $m_{OA}(0) = m_R(0)$, one may write:

$$\mathrm{MLR} = \frac{\Delta m_{OA}}{\Delta m_R} = \frac{m_{OA} - m_{OA}(0)}{m_R - m_R(0)} = \frac{1-\mu_{OA}}{1-\mu_R} \quad (2)$$

where μ is the mass fraction remaining of either total aerosol or the reactive species. For our purposes, we assume that $\mu_R = m_j / m_j(0)$, where m_j is the mass of the selected AMS peak as computed in Equation 1. The MLR therefore describes the approximate yield of gas-phase products upon oxidation. Values of the MLR are determined by averaging all data points for which the total particle mass loss is greater than 20%, since values computed at low-oxidation conditions are subject to substantial numerical errors.

We characterize the chemical changes to the reacting systems in terms of changes to the overall elemental composition of organics in the condensed phase. In particular, the oxygen-to-carbon ratio (O/C) and hydrogen-to-carbon ratio (H/C) are combined to estimate the overall degree of oxidation of OA particles and the relative contributions of key functional groups. The method for calculating elemental ratios from high-resolution AMS data is described in detail by Aiken et al. (*18*,*19*). This approach requires a set of factors to correct measured values for biases

in ion fragmentation. Such factors are expected to be most accurate for complex mixtures or organics, such as are found in ambient OA. As noted by Aiken et al. (*18*,*19*), these standard correction factors (0.75 for O/C and 0.91 for H/C), are not as accurate for the measurement of individual organics, such as those studied in the present experiments. We therefore use system-specific correction factors for these studies in order to ensure that the elemental ratios of pure compounds are reported as their known values. The correction factors used are 0.44 for O/C and 0.82 for H/C for erythritol, and 0.50 for O/C and 1.1 for H/C for levoglucosan, which is similar to the correction for pure levoglucosan reported previously (*18*). Regardless of the correction factor used, the overall conclusions reached with respect to the oxidative mechanism described below remain unchanged.

IV. Results

Sample mass spectra of erythritol and levoglucosan particles at both low and high OH exposures may be found in Figure S-6 and demonstrate significant changes in particle mass and chemical characterization.

(i) Erythritol

Figure 1a depicts the decay rates of both erythritol and total particle mass for the heterogeneous oxidation of pure erythritol particles (surface-weighted mean diameter: 270.5 nm). The exponential decay of erythritol is consistent with a pseudo-first-order approximation of the second-order reaction of organic compounds with OH, although the chosen marker peak ($C_4H_8O_3^+$) does not appear to decay to zero. Possible reasons for this apparent offset include unreacted erythritol in the core of the particles (with a slow mass transfer rate) and signal interference from product compounds at the marker peak. A fit to the first e-fold of the decay is therefore used (Figure S-1) to obtain a rate constant of $(2.54 \pm 0.22) \times 10^{-13}$ cm^3 molecule^{-1} s$^-$

[1]. The mass loss ratio, a measure of the formation of gas- versus particle-phase reaction products (Equation 2), is computed to be 0.75 ± 0.04. Thus the heterogeneous oxidation of erythritol leads primarily to the formation of volatile products (~75% yield), which escape into the gas phase. Reported errors reflect uncertainty in the AMS peak calculation, SMPS mass, and fluctuations in the atomizer flow and OH concentration within the reactor.

Heterogeneous oxidation kinetics can be described in terms of the effective uptake coefficient $\gamma_{i,\mathrm{OH}}$ defined as the ratio of the number of reactive collisions between OH and the compound of interest to the total number of collisions (*5*). The uptake coefficient may be calculated from the determined second-order rate constant according to

$$\gamma_{i,\mathrm{OH}} = \frac{2D_0 \cdot \rho_i \cdot N_A}{3\bar{c}_{\mathrm{OH}} \cdot M_i} \cdot k_{i,\mathrm{OH}} \quad (3)$$

where D_0 is the surface-weighted average particle diameter at the start of the experiment, ρ_i is the density of the organic compound, N_A is Avogadro's number, $\bar{c}_{\mathrm{OH}}$ is the average speed of hydroxyl radicals in the gas phase, and M_i is the molecular weight of the compound. The uptake coefficient calculated by this method for erythritol, after correcting for diffusion limitations (which account for approximately a 40% difference in the final value, using a diffusion constant of OH in air of 0.217 $cm^2\ s^{-1}$) (*5*,*20*), is 0.85 ± 0.12. Equation 3 is exact for spherical particles and may slightly overestimate $\gamma_{i,\mathrm{OH}}$ for particles with higher surface-area to volume ratios.

Figure 1b shows the evolution of three selected fragment ion signals from the AMS (each normalized to its maximum value) with increasing oxidant exposure. As in Figure 1a, the amount of erythritol remaining is represented by its marker ion, $C_4H_8O_3^+$. Additionally, we use $C_4H_7O_3^+$ (*m/z* = 103, M-19) as a marker for first-generation oxidation products; the signal from

this ion is negligible for pure erythritol compared with its observed rise in the reacting system. While the choice of marker peak is determined on a largely empirical basis, it should be noted that if we assume that each oxidation reaction involves the formation of a carbonyl, either by addition or by conversion of a hydroxyl group and requiring the loss of two hydrogen atoms (as discussed in the next section), higher-generation products would necessarily have 6 or fewer hydrogen atoms and would therefore be unable to form the $C_4H_7O_3^+$ fragment ion. We are therefore confident that the selected ion peak serves as a useful metric for the formation of first-generation products.

The rate coefficient computed for the decay of erythritol is combined with a simplified two-step oxidation model (described in detail in the Supporting Information) in order to estimate a rate coefficient for the decay of first-generation products, with the fit trace shown in Figure 1b. The resulting effective uptake coefficient is calculated by equation 3 as 0.28 ± 0.03, significantly less than that of its parent compound, erythritol. Lastly, CO_2^+ (m/z = 44) is taken to be representative of the most highly oxidized compounds present in the mixture, likely indicating the presence of carboxylic acid groups in product molecules; additional discussion of changes in the CO_2^+ presence may be found in the Supporting Information. The calculated decay of first-generation products and apparent subsequent growth of more oxidized compounds together indicate that heterogeneous oxidation is a multigenerational process, in accord with previous results (*5*), and points to the continually evolving chemical nature of OA, which is consistent with a recent study of the heterogeneous oxidation of SOA (*21*).

Figure 1c shows the elemental ratios O/C and H/C for the particulate products of OH + erythritol. Although the relative amount of oxygen in erythritol particles rises only slightly, the hydrogen content drops by a significant degree over the course of the reaction, suggesting that

206 the dominant reactions that yield condensed-phase products are likely to involve the conversion
207 of hydroxyl groups to carbonyl groups. The slight increase in O/C can be accounted for in part
208 by the growing CO_2^+ signal (to a maximum of ~6% of the AMS organic signal), which suggests
209 the increased importance of carboxylic acid functional groups as well.
210 *(ii.) Levoglucosan*
211 The levoglucosan oxidation experiments were analyzed using the same approach as used
212 for erythritol, described above; results are presented in the right half of Figure 1. Figure 1d
213 depicts the decay rates of both levoglucosan mass and total particle mass in a system initially
214 containing pure levoglucosan particles (surface-weighted mean diameter: 304.3 nm). The
215 exponential decay is again consistent with a second-order reaction model and has a
216 corresponding rate constant of $(3.09 \pm 0.18) \times 10^{-13}$ cm^3 $molecule^{-1}$ s^{-1}, with a diffusion-
217 corrected effective uptake coefficient of 1.05 ± 0.11. Although this computed value is greater
218 than unity, errors caused by under-estimating the average particle surface area using the mobility
219 diameter may lower the actual value. The mass loss ratio, determined by equation 2, is 0.23 ±
220 0.04, significantly lower than what was observed for erythritol. This indicates that the majority
221 of the products of levoglucosan oxidation remain in the particle phase. Hennigan et al. have
222 reported a similar effect, whereby mass loss of biomass-burning organic aerosol upon oxidation
223 is much slower than the loss rate of levoglucosan (*10*).
224 Figure 1e depicts the progression of selected marker ion peaks with increasing oxidant
225 exposure. Levoglucosan is represented by $C_6H_8O_4^+$, first-generation products are denoted by
226 $C_6H_7O_4^+$ (*m/z* = 143, M-19), and the most highly oxidized compounds are monitored by CO_2^+.
227 The selection of these three ion peaks follows the same process as described for erythritol in

Figure 1b. Again, the growth and subsequent decay of first-generation products, coupled with the later rise in CO_2^+ signal, presents evidence of significant multigenerational chemistry on atmospherically relevant oxidation timescales. The effective uptake coefficient for product decay is calculated to be 0.39 ± 0.05, a similar effect to the one observed in the erythritol oxidation system, and fit traces for both levoglucosan and its products are indicated in Figure 1e as well.

Levoglucosan undergoes a drop in H/C similar to erythritol, as shown in Figure 1f, but the larger rise in O/C suggests that oxidation reactions also involve the addition of new functional groups, such as hydroxyl, carbonyl, and carboxylic acid groups (CO_2^+ signal reaches ~8% of the total AMS organic signal), instead of solely the conversion of alcohols to carbonyls. As oxidant exposure increases, the values of O/C of both systems begin to converge to an apparent upper bound of ~1.1.

V. Discussion

(i.) Oxidative mechanisms & Structural effects

In marked contrast to the heterogeneous oxidation of reduced particulate organics (*2*,*3*,*5*), the heterogeneous oxidation of erythritol and levoglucosan leads to a substantial loss of OA mass via volatilization reactions. The differences in the mass loss plots of erythritol and levoglucosan (Figures 1a and 1d, respectively) indicate that the effects of oxidation on aerosol loadings are highly dependent on the chemical structure of the organic species in the aerosol. Although the two compounds decay at very similar rates—the effective uptake coefficients γ agree to within approximate experimental uncertainty—the total particle mass follows this decay much more closely for erythritol than it does for levoglucosan. This discrepency likely arises from differences in the chemical mechanisms leading to volatility changes.

These differences can be understood in terms of the mechanism of the oxidation of polyols, depicted in Figure 2 (*22*). In pathway A, abstraction of a hydrogen atom from a carbon bonded to a hydroxyl group, followed by reaction with O_2, leads to the direct formation of a carbonyl without the cleavage of a C-C bond. In pathway B, the hydrogen atom is instead abstracted from the hydroxyl group directly. The resulting α-hydroxy alkoxy radical rapidly decomposes by C-C bond scission. While the former case raises product vapor pressure by approximately one order of magnitude (*23*), the latter may raise volatility by a much larger degree by decreasing the carbon number of each product molecule. However, in the case of cyclic molecules, "tethering" of the R groups allow for the cleavage of a C-C bond with no change to the carbon number. Levoglucosan, which has two cyclic moieties, can therefore undergo two cleavage reactions without dissociating to two separate molecules and so will not experience as dramatic an increase in vapor pressure as erythritol. The rate of mass loss relative to oxidation is therefore lower, suggesting that compounds with ring structures and higher molecular weights are likely to contribute to longer-lived organic aerosol.

Because both compounds are polyhydroxylated, similar pathways to those discussed above are possible for successive generations of oxidative reactions. The low decay rate of first-generation products in both systems—relative to the decay rate of initial compound—indicates, however, that the reaction process is demonstrably slowed, in part by the loss of hydrogen atoms needed for abstraction in the first step of oxidation. Although some degree of the difference in reaction rates can be explained by the changing sphericity of particles with increasing oxidation, conservative estimates of the uptake coefficient still yield significant discrepancies between the decay rates of initial compounds and the decay of first-generation products. Additionally, the growing presence of the CO_2^+ ion in both systems points to the likely production of carboxylic

acid groups upon later generations of oxidation; this is consistent with our recent evidence that carboxylic acid addition becomes increasingly important with fragmentation reactions (*4*), although the detailed mechanisms are not yet well understood.

(ii.) Van Krevelen Analysis

The direct comparison of elemental ratios, independent of time or oxidant exposure, is made in Figure 3, using a "van Krevelen diagram" (a plot of H/C vs O/C) (*24*,*25*). Heald et al. recently showed that for many ambient measurements of OA, as well as for several laboratory oxidation studies, elemental ratio data tend to fall along a line passing through (0,2) and with a slope of about -1 in this space, consistent with a mixture of carbonyl- and hydroxyl-forming reactions during oxidative aging (*24*). As shown in Figure 3, erythritol and levoglucosan are located at points far away from this line. As the particles are exposed to larger amounts of OH, the particulate organics tend strongly downwards, with an approximate slope of -4.6 for erythritol and -1.3 for levoglucosan. The steeper slope for erythritol is a result of the conversion of hydroxyl groups to carbonyl groups. Both systems are moving towards similar C/H/O relationships, consistent with previous observations that oxidative aging of widely varying organics tends to form products with similar chemical properties (*1*).

The chemical information supplied by a system's coordinates on a van Krevelen diagram is sufficient to estimate the minimum number of carbon atoms that a compound must have to be found predominantly in the particle phase at a given loading. These are determined by assuming that compounds are composed solely of contiguous saturated carbon chains and have only hydroxyl and carbonyl (and, by extension, carboxylic acid) functional groups. Volatilities are calculated using the group contribution method of Pankow and Asher (*23*), and the carbon

number represents the minimum number of carbon atoms required to ensure that the compound will partition by at least one-half into the condensed phase (*26*).

The shaded regions in Figure 3a represent the minimum carbon number calculated over the entire range of realistic O/C and H/C values for a system in which the aerosol loading is 700 μg m^{-3}, the approximate loading in the present experiments. The data for both erythritol (four carbons) and levoglucosan (six carbons) remain within the prescribed limits for condensed-phase elemental composition, indicating consistency between the estimated volatilities of organic compounds and the present measurements. However, because each point on the diagram represents an average in terms of the elemental composition of the system, individual products may be further removed from the observed data, leading to significant phase partitioning of some highly oxidized compounds.

(iii.) Atmospheric Implications

Although Figure 3a is sufficient to describe the phase partitioning behavior of compounds in the present experiments, the aerosol loadings studied are 1-3 orders of magnitude greater than typical ambient loadings (*1*). We correct for this in Figure 3b, which adjusts the contours to correspond to a loading of 10 μg m^{-3}. In this case, levoglucosan and its immediate oxidation products are still expected to remain largely within the condensed phase during aging. The erythritol system, however, moves rapidly into a region for which four carbon units is insufficient to ensure that oxidation products will be present primarily in the particle phase. Many of the condensed-phase products observed in this experiment are therefore likely to become even more strongly volatilized in the atmosphere, so that the mass loss ratio is likely to increase as the atmospheric OA loading becomes more dilute; this observation underscores the

317 importance of volatility changes arising from interconversion of functional groups upon
318 oxidation.

319 The effective uptake coefficient can be combined with estimates of particle size and
320 atmospheric oxidant concentration in order to determine a pseudo-first-order rate coefficient for
321 the compound of interest and, by extension, the compound's atmospheric lifetime. Assuming a
322 mean diameter of ~200 nm and OH concentration of 3×10^6 molecules cm^{-1}, erythritol would
323 have a heterogeneous oxidation lifetime of about 12.7 days, while levoglucosan would have a
324 lifetime of about 9.6 days, both of which are very near the estimated depositional lifetimes (~10
325 days) of similarly-sized particles (*27*). Whereas previous studies have suggested that
326 heterogeneous oxidation of reduced organics (hydrocarbons) (*2*,*3*,*5*) and some SOA systems (*21*)
327 does not significantly affect aerosol mass on atmospherically relevant timescales, the much
328 lower lifetimes determined here for levoglucosan and erythritol suggest that mass changes from
329 heterogeneous reactions may be more significant for compounds that are already more heavily
330 oxidized and have low molecular weights, which is consistent with our recent results (*4*).
331 Additional studies have shown that in aqueous droplets and environments with high relative
332 humidity, the lifetimes of both compounds are decreased to less than a day (*10*,*11*,*12*). It should
333 also be noted that because erythritol is semi-volatile, gas-phase oxidation reactions are likely to
334 represent an even larger atmospheric sink for the compound in regions with low-to-moderate OA
335 loadings; this may partially explain previous observations of a decrease in isoprene SOA mass by
336 further aging (*28*).

337 The chemical lifetimes of OA mass contributed by these compounds—comprising the
338 initial compound and its condensed-phase oxidation products—may be estimated approximately
339 by dividing the product lifetime by its mass loss ratio. Since the mass loss ratio of erythritol

approaches unity at atmospheric conditions, its OA lifetime will be about the same as that of erythritol (~12.7 days), suggesting oxidative aging could in fact be an important sink of polyhydroxylated (and possibly other oxidized) components of OA, though the secondary effects of more complex aerosol mixtures on oxidation remains an important topic for further research. The low observed MLR of levoglucosan, by contrast, implies longer-lived particle-phase products, on the order of several weeks, although OA continues to be slowly volatilized during this time. We therefore demonstrate that oxidized organic compounds found in both SOA and BBOA—which make up a large fraction of total aerosol loading (*1*)—are susceptible to further heterogeneous oxidation reactions and that these reactions are capable of significantly altering both the chemical composition and the mass of the oxidized OA.

VI. References

(1) Jimenez, J. L. et al. Evolution of organic aerosols in the atmosphere. *Science* **2009**, *326*, 1525.

(2) George, I. J.; Vlasenko, A.; Slowik, J. G.; Broekhuizen, K.; Abbatt, J. P. Heterogeneous oxidation of saturated organic aerosols by hydroxyl radicals: uptake kinetics, condensed-phase products, and particle size change. *Atmospheric Chemistry and Physics* **2007**, *7*, 4187–4201.

(3) Hearn, J. D.; Renbaum, L. H.; Wang, X.; Smith, G. D. Kinetics and products from reaction of Cl radicals with dioctyl sebacate (DOS) particles in O_2: a model for radical-initiated oxidation of organic aerosols. *Physical Chemistry Chemical Physics* **2007**, *9*, 4803–4813.

(4) Kroll, J.; Smith, J.; Che, D.; Kessler, S.; Worsnop, D.; Wilson, K. Measurement of fragmentation and functionalization pathways in the heterogeneous oxidation of oxidized organic aerosol. *Physical Chemistry Chemical Physics* **2009**, *11*, 8005–8014.

(5) Smith, J. D.; Kroll, J. H.; Cappa, C. D.; Che, D. L.; Liu, C. L.; Ahmed, M.; Leone, S. R.; Worsnop, D. R.; Wilson, K. R. The heterogeneous reaction of hydroxyl radicals with sub-micron squalane particles: a model system for understanding the oxidative aging of ambient aerosols. *Atmospheric Chemistry and Physics* **2009**, *9*, 3945–3981.

(6) Rudich, Y.; Donahue, N. M.; Mentel, T. F. Aging of Organic Aerosol: Bridging the Gap Between Laboratory and Field Studies. *Annual Review of Physical Chemistry* **2007**, *58*, 321-352.

(7) Claeys, M.; Graham, B.; Vas, G.; Wang, W.; Vermeylen, R.; Pashynska, V.; Cafmeyer, J.; Guyon, P.; Andreae, M. O.; Artaxo, P.; Maenhaut, W. Formation of Secondary Organic Aerosols Through Photooxidation of Isoprene. *Science* **2004**, *303*, 1173-1176.

(8) Surratt, J. D.; Murphy, S. M.; Kroll, J. H.; Ng, N. L.; Hildebrandt, L.; Sorooshian, A.; Szmigielski, R.; Vermeylen, R.; Maenhaut, W.; Claeys, M.; Flagan, R. C.; Seinfeld, J. H. Chemical Composition of Secondary Organic Aerosol Formed from the Photooxidation of Isoprene. *The Journal of Physical Chemistry A* **2006**, *110*, 9665-9690.

(9) Simoneit, B. R.; Schauer, J. J.; Nolte, C. G.; Oros, D. R.; Elias, V. O.; Fraser, M. P.; Rogge, W. F.; Cass, G. R. Levoglucosan, a tracer for cellulose in biomass burning and atmospheric particles. *Atmospheric Environment* **1999**, *33*, 173–182.

(10) Hennigan, C. J.; Sullivan, A. P.; Collett, Jr., J. L.; Robinson, A. L. Levoglucosan Stability in Biomass Burning Particles Exposed to Hydroxyl Radicals. *Geophysical Research Letters* **2010** doi: 10.1029/2010GL043088.

(11) Hoffmann, D.; Tilgner, A.; Iinuma, Y.; Herrmann, H. Atmospheric stability of levoglucosan: a detailed laboratory and modeling study. *Environmental science & technology* **2010**, *44*, 694-9.

(12) Hoffmann, D.; Weigert, B.; Barzaghi, P.; Herrmann, H. Reactivity of poly-alcohols towards OH, NO_3 and SO_4^- in aqueous solution. *Physical Chemistry Chemical Physics* **2009**, *11*, 9351-9363.

(13) Kleindienst, T. E.; Jaoui, M.; Lewandowski, M.; Offenberg, J. H.; Lewis, C. W.; Bhave, P. V.; Edney, E. O. Estimates of the contributions of biogenic and anthropogenic hydrocarbons to secondary organic aerosol at a southeastern US location. *Atmospheric Environment* **2007**, *41*, 8288-8300.

(14) Molina, M.; Ivanov, A.; Trakhtenberg, S.; Molina, L. Atmospheric evolution of organic aerosol. *Geophys. Res. Lett* **2004**, *31*, 22 doi:10.1029/2004GL020910.

(15) Rissman, T. A.; Varutbangkul, V.; Surratt, J. D.; Topping, D. O.; McFiggans, G.; Flagan, R. C.; Seinfeld, J. H. Cloud condensation nucleus (CCN) behavior of organic aerosol particles generated by atomization of water and methanol solutions. *Atmospheric Chemistry and Physics Discussions* **2006**, *6*, 13251–13305.

(16) Dixon, R. W.; Baltzell, G. Determination of levoglucosan in atmospheric aerosols using high performance liquid chromatography with aerosol charge detection. *Journal of Chromatography A* **2006**, *1109*, 214-221.

(17) DeCarlo, P.; Slowik, J. G.; Worsnop, D. R.; Davidovits, P.; Jimenez, J. L. Particle morphology and density characterization by combined mobility and aerodynamic diameter measurements. Part 1: Theory. *Aerosol Science and Technology* **2004**, *38*, 1185–1205.

(18) Aiken, A. C.; DeCarlo, P. F.; Jimenez, J. L. Elemental analysis of organic species with electron ionization high-resolution mass spectrometry. *Anal. Chem* **2007**, *79*, 8350–8358.

(19) Aiken, A. C. et al. O/C and OM/OC ratios of primary, secondary, and ambient organic aerosols with high-resolution time-of-flight aerosol mass spectrometry. *Environ. Sci. Technol* **2008**, *42*, 4478–4485.

(20) Fuchs, N. A.; Sutugin, A. G. Highly dispersed aerosols. *Highly dispersed aerosols*; Halsted Press, New York, 1970.

(21) George, I. J.; Abbatt, J. P. Chemical evolution of secondary organic aerosol from OH-initiated heterogeneous oxidation. *Atmospheric Chemistry and Physics* **2010**, *10*, 3265-3300.

(22) Bethel, H. L.; Atkinson, R.; Arey, J. Hydroxycarbonyl Products of the Reactions of Selected Diols with the OH Radical. *The Journal of Physical Chemistry A* **2003**, *107*, 6200-6205.

(23) Pankow, J. F.; Asher, W. E. SIMPOL. 1: a simple group contribution method for predicting vapor pressures and enthalpies of vaporization of multifunctional organic compounds. *Atmos. Chem. Phys* **2008**, *8*, 2773–2796.

(24) Heald, C. L.; Kroll, J. H.; Jimenez, J. L.; Docherty, K. S.; DeCarlo, P. F.; Aiken, A. C.; Chen, Q.; Martin, S. T.; Farmer, D. K.; Artaxo, P. A simplified description of the evolution of organic aerosol composition in the atmosphere. *Geophysical Research Letters* **2010**, *37* doi:10.1029/2010GL042737.

(25) Walser, M. L.; Desyaterik, Y.; Laskin, J.; Laskin, A.; Nizkorodov, S. A. High-resolution mass spectrometric analysis of secondary organic aerosol produced by ozonation of limonene. *Physical Chemistry Chemical Physics* **2008**, *10*, 1009-1022.

(26) Donahue, N. M.; Robinson, A. L.; Stanier, C. O.; Pandis, S. N. Coupled Partitioning, Dilution, and Chemical Aging of Semivolatile Organics. *Environmental Science & Technology* **2006**, *40*, 2635-2643.

(27) Kanakidou, M. et al. Organic aerosol and global climate modelling: a review. *Atmospheric Chemistry and Physics* **2005**, *5*, 1053–1123.

(28) Kroll, J. H.; Ng, N. L.; Murphy, S. M.; Flagan, R. C.; Seinfeld, J. H. Secondary Organic Aerosol Formation from Isoprene Photooxidation. *Environmental Science & Technology* **2006**, *40*, 1869-1877.

433

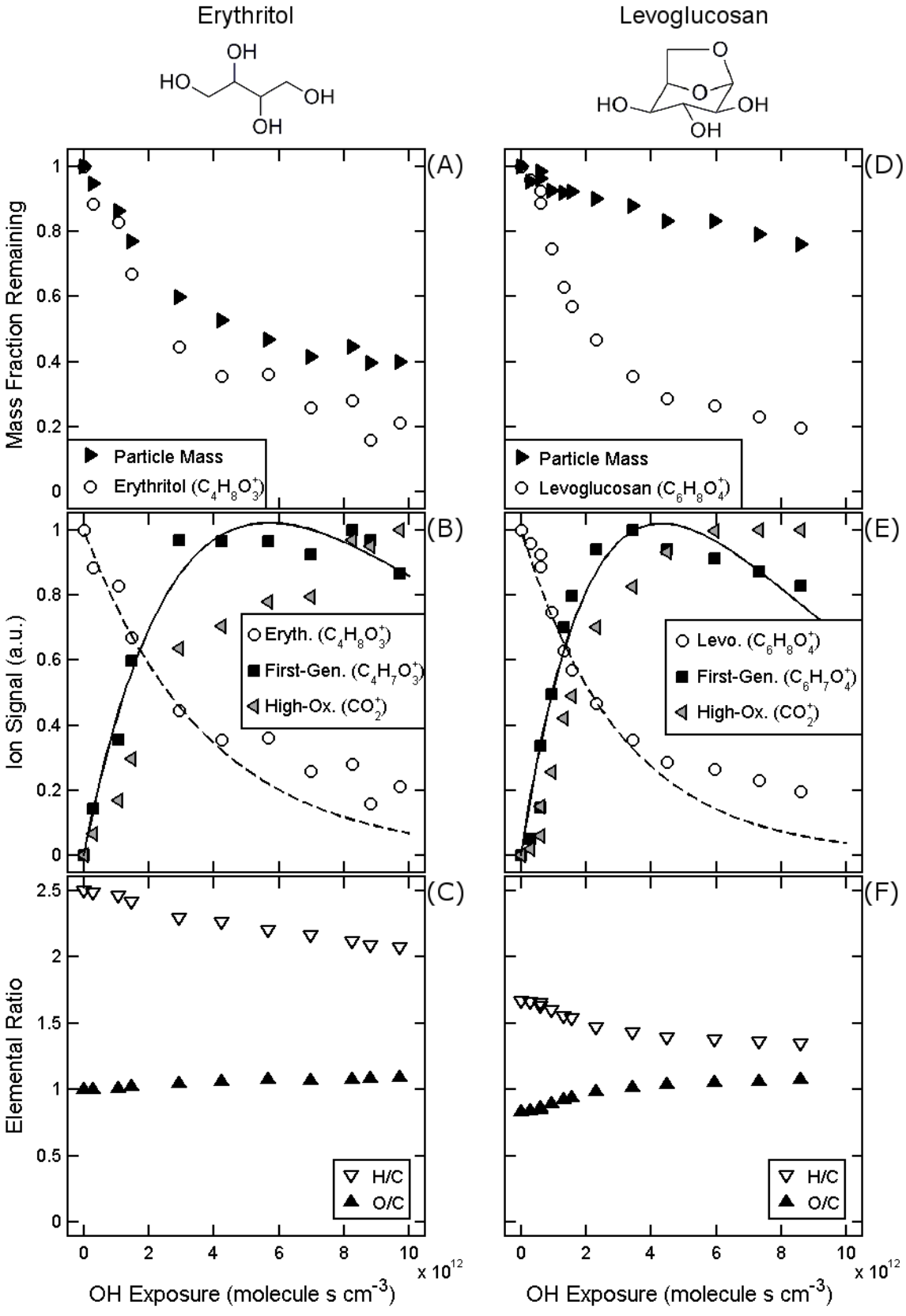
Erythritol
Levoglucosan
(A)
(B)
(C)
(D)
(E)
(F)
Mass Fraction Remaining
Ion Signal (a.u.)
Elemental Ratio
Particle Mass
Erythritol ($C_4H_8O_3^+$)
Levoglucosan ($C_6H_8O_4^+$)
Eryth. ($C_4H_8O_3^+$)
Levo. ($C_6H_8O_4^+$)
First-Gen. ($C_4H_7O_3^+$)
First-Gen. ($C_6H_7O_4^+$)
High-Ox. (CO_2^+)
H/C
O/C
x 10^{12}
OH Exposure (molecule s cm^{-3})

434

Figure 1. (A) Decay curves of pure erythritol (open circles) and total particle mass (filled triangles) over increasing oxidant exposures. (B) Mass contributions of selected marker peaks, used to represent erythritol (circles), first-generation products (squares), and heavily-oxidized products (triangles). Solid and dashed curves denote non-linear fits to kinetic expressions. (C) Hydrogen-to-carbon (H/C, open triangles) and oxygen-to-carbon (O/C, filled triangles) ratios of reacted erythritol system. (D-F) Structure and evolving characteristics of levoglucosan system, as compared to erythritol.

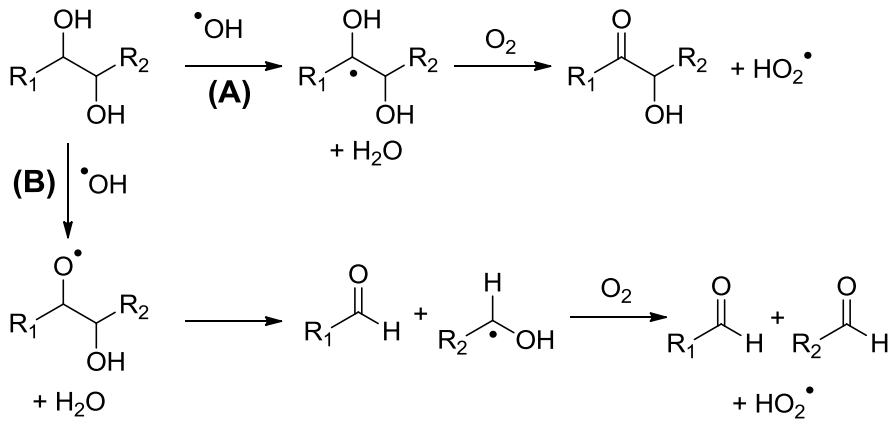

Figure 2. Two possible reaction pathways in the oxidation of erythritol and levoglucosan, adapted from Bethel et al. (*22*). The functionalization pathway (A) leads to a higher degree of oxidation without resulting in the loss of carbon, but the conversion of a hydroxyl group to a carbonyl group results in a product of higher volatility. The fragmentation pathway (B) leads to degradation of C-C bonds and strongly increases overall particle volatility. If the two R groups are connected to each other, however, the molecular backbone will remain intact, and volatilization will be suppressed.

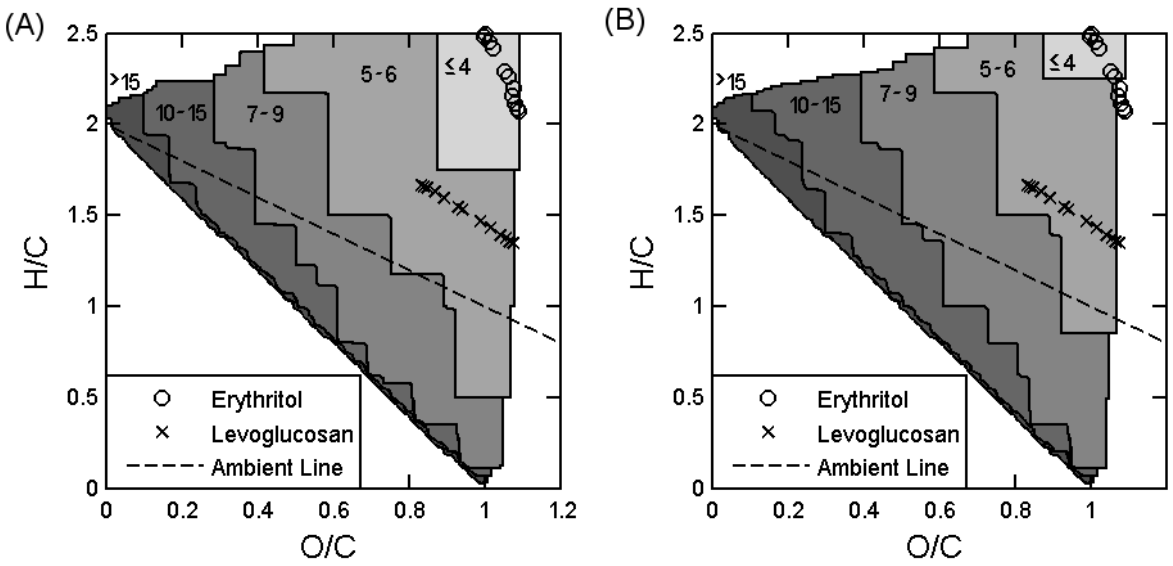

Figure 3. (A) Van Krevelen plot of H/C versus O/C for the erythritol (circles) and levoglucosan ('x') reacting systems. The direction of oxidation is downward and to the right for each system. Dashed line depicts the "ambient" line (H/C = 2 – O/C), which is the average of many measurements. Shaded regions represent the approximate minimum number of carbon atoms per molecule required in order for the compounds to have a saturation concentration less than 700 µg m^{-3}, the approximate mass loading of the systems considered herein. Blank spaces represent regions for which the calculated minimum carbon number, along with the represented hydrogen and oxygen numbers, result in chemically infeasible combinations in the absence of carbon-carbon double bonds. (B) The same Van Krevelen plot, with shaded regions adjusted to the more atmospherically-relevant loading of 10 µg m^{-3}. The erythritol system average moves out of the "4-carbon" region at an OH exposure of 4×10^{12} molecule s cm^{-3}, corresponding to ~15.4 days of oxidation in the atmosphere.